

Symmetry analysis of possible superconducting states in $K_x\text{Fe}_2\text{Se}_2$ superconductors

I.I. Mazin

Code 6393, Naval Research Laboratory, Washington, DC 20375, USA

A newly discovered family of the Fe-based superconductors is isostructural with the so-called 122 family of Fe pnictides, but has a qualitatively different doping state. Early experiments indicate that superconductivity is nodeless, yet prerequisites for the s_{\pm} nodeless state (generally believed to be realized in Fe superconductors) are missing. It is tempting to assign a d -wave symmetry to the new materials, and it does seem at first glance that such a state may be nodeless. Yet a more careful analysis shows that it is not possible, given the particular 122 crystallography, and that the possible choice of admissible symmetries is severely limited: it is either a conventional single-sign s_{+} state, or another s_{\pm} state, different from the one believed to be present in other Fe-based superconductors.

PACS numbers: 74.20.Pq, 74.25.Jb, 74.70.Xa

Recent reports of superconductivity at T_c in excess of 35 K¹ in Se-based iron superconductors (FeBS) isostructural with BaFe_2As_2 (the so-called 122 structure) have triggered a new surge of interest among the physics community. These materials are believed by many to open a new page in Fe-based superconductivity. Indeed, the formal composition, AFe_2Se_2 , where A is an alkali metal, corresponds to a formal doping of 0.5 electron off the standard for FeBS parent compounds (LaFeAsO , BaFe_2As_2 , or FeSe) valence state of iron, Fe^{2+} . Such a large doping in other materials, such as $\text{Ba}(\text{Fe},\text{Co})_2\text{As}_2$ leads to a complete suppression of superconductivity, which has been generally ascribed^{2,3} to disappearance of the hole pockets of the Fermi surface and formal violation of the quasinesting condition for the s_{\pm} superconductivity.

Indeed all band structure calculations show⁴ that in AFe_2Se_2 the hole bands are well under the Fermi surface (for the reported experimental crystal structure of KFe_2Se_2 , about 60 meV), and this is confirmed by preliminary ARPES results⁵⁻⁷. This has led to speculations that in this subfamily it is not the familiar s_{\pm} superconductivity that is realized, but a d -wave superconductivity^{5,8-10} of the sort discussed in an early paper by Kuroki *et al*¹¹. Unfortunately, these speculations are entirely based upon the “unfolded” Brillouin zone description of the electronic structure, a simplified model that neglects the symmetry lowering due to the As or Se atoms and the fact that in the real unit cell there are two Fe ions, and not one. Furthermore they implicitly assume that spin susceptibility corresponding to the “checkerboard” wave vector, $Q = (\pi, \pi)$, is substantially enhanced, despite the fact that this vector corresponds to an electron-electron interband transition that is much less efficient in enhancing susceptibility (here and below, we used the bar when we work in the unfolded Brillouin zone). This assumption is supported by model calculations based on an onsite Hubbard Hamiltonian⁸, but its applicability to FeBS is still an open question.

In this paper, we will critically address these two assumptions, and will show that the latter assumption is supported by first principles calculations, but the former assumption is actually very misleading. We will present

a general symmetry analysis of possible superconducting symmetries supported by the Fermi surface topology existing in AFe_2Se_2 . This analysis is not limited by a specific density functional calculation, but is based on the general crystallographic considerations appropriate for this crystal structure. It appears that it is impossible to fold down a nodeless d -wave state so as to avoid formation of line nodes. Thus, emerging experimental evidence from ARPES⁵⁻⁷, specific heat¹², NMR¹³, and optics¹⁴ that superconductivity in AFe_2Se_2 is nodeless is a strong argument against d -wave. A conventional s -state is also unlikely based on the proximity to magnetism and actual observation of a coexistence of superconductivity and magnetism. We emphasize that the symmetry of the folded Fermi surfaces does allow for a nodeless state, which however has an overall s symmetry and can also be called s_{\pm} , as it is strongly sign-changing. Unlike the s_{\pm} advocated for the “old” FeBS it is not driven by $(\pi, 0)$ spin fluctuations and cannot be derived from considering an unfolded Brillouin zone Fermi surface.

The unfolded Fermi surface topology in materials with the 122 structure is controlled by two factors: ellipticity of individual electron pockets and their k_z dispersion (Fig. 1). The ellipticity in the unfolded zone is determined by the relative position of the xy and xz/yz levels of Fe, and the relative dispersion of the bands derived from them. Indeed¹⁵, the point on the Fermi surface located between $\bar{\Gamma}$ and \bar{X} has a purely xy character, while that between $\bar{\Gamma}$ and \bar{M} a pure yz character. At the \bar{X} point the xy state is slightly below the yz state, but has a stronger dispersion, therefore depending on the system parameters and the Fermi level the corresponding point of the Fermi surface may be more removed from \bar{X} , or less. In the 1111 compounds, the first to have been investigated, the dispersion of the xy band is not high enough to reverse the natural trend, so the Fermi surface remains elongated in the $\bar{\Gamma}\bar{X}$ (1,0) direction.

For both xy and xz/yz bands the hopping mainly proceeds via As (Se) p -orbitals. The xy states mainly hop through the p_z orbital (see Ref.¹⁶ for more detailed discussions), and xz (yz) via p_y (p_x) orbitals. If there is a considerable interlayer hopping between the p orbitals, whether direct (11 family) or assisted (122 family), the

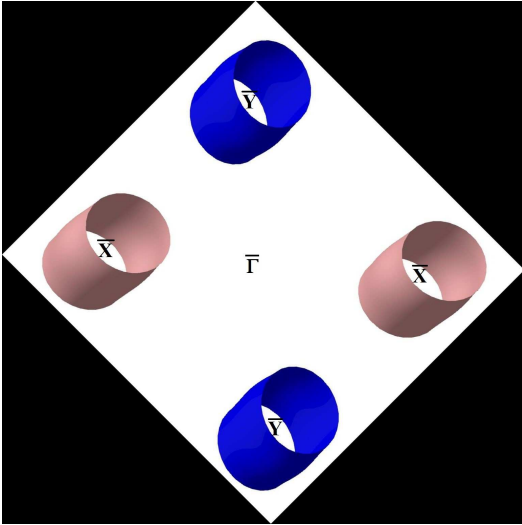


FIG. 1. A cartoon showing a generic 3D Fermi surface for an AFe_2Se_2 material in the unfolded (one Fe/cell) Brillouin zone. Different colors show the signs of the order parameter in a nodeless d -wave state, allowed in the unfolded zone. The Γ point is in the center (no Fermi surface pockets around Γ), and the electron pockets are around the \bar{X}, \bar{Y} points.

ellipticity becomes k_z -dependent. For instance, in FeSe there is noticeable overlap between the Se p_z orbitals, so that they form a dispersive band with the maximum at $k_z = 0$ and the minimum at $k_z = \pi/c$. Obviously, hybridization is stronger when the p_z states are higher, therefore the Fermi surface ellipticity is completely suppressed in the $k_z=0$ plane, while rather strong in the $k_z = \pi/c$ plane, which leads to formation of the characteristic “bellies” in the Fermi surface of FeSe. On the other hand, $p_{x,y}$ orbitals in FeSe do not overlap in the neighboring layers, so the xz and yz bands have very little k_z dispersion, so that the inner barrels of the electronic pockets in this compound are practically 2D.

In 122, the interlayer hopping proceeds mainly via the Ba (K) sites, and thus the k_z dispersion is comparable (but opposite in sign!) for the xy and xz/yz bands. As a result, when going from the $k_z = 0$ plane to the $k_z = \pi/c$ plane the longer axis of the Fermi pocket shrinks, and the shorter expands, so that the ellipticity actually changes sign.

Importantly, the symmetry operation that folds down the single-Fe Brillouin zone when the unit cell is doubled according to the As (Se) site symmetry is different in the 11 and 1111 structures, as compared to the 122 structure. In the former case, the operation in question is the translation by $(\bar{\pi}, \bar{\pi}, 0)$, without any shift in the k_z direction, in the latter by $(\bar{\pi}, \bar{\pi}, \bar{\pi})$. Thus the folded Fermi surface in 11 and in 1111 has full fourfold symmetry, while that in the 122 has such symmetry only for one particular k_z , namely $k_z = \pi/2c$. Furthermore, in 122 the folded bands are not degenerate along the MX (now the labels are without the bars, that is, corresponding to the folded BZ), as they were in 11/1111. Finally, there is a

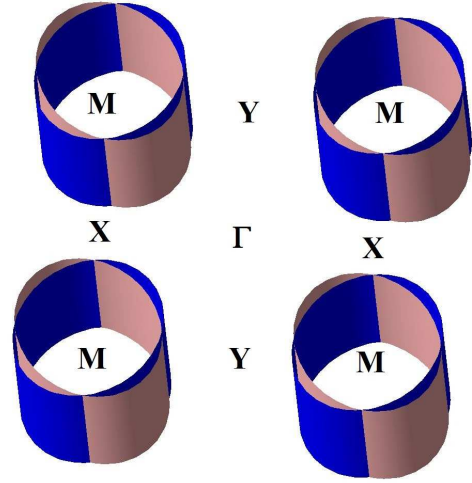


FIG. 2. A cartoon showing a folded 3D Fermi surface for an AFe_2Se_2 material, assuming a finite ellipticity, but zero k_z dispersion. Different colors show the signs of the order parameter in a d -wave state. Wherever the two colors meet, turning on hybridization due to the Se potential creates nodes in the order parameter.

considerable (at least on the scale of the superconducting gap) hybridization when the folded bands cross (except for $k_z = 0$).

Now we are ready to analyze possible superconducting symmetries in the actual AFe_2Se_2 materials. We shall not adhere strictly to the calculated band structure and the Fermi surfaces, but rather consider several possibilities allowed by symmetry. Let us start first from a d -wave state in the unfolded BZ, as derived in Refs.^{8,9,11}. In Fig. 1 we show by the two colors the signs of the order parameter. Obviously in the *unfolded* BZ such a state has no nodes.

Let us now assume that the k_z dispersion is negligible, while the ellipticity remains finite. After folding, but before turning on the hybridization, we have the picture shown in Fig. 2. The border between the red and the blue colored regions now becomes a nodal line¹⁷. In this case, we have four such lines for each pair of electron pockets. One can think of an effective “thickness” of the nodal lines, meaning the distance in the momentum space over which the sign of the order parameter changes. This is defined by the ratio of the hybridization gap at the point where the bands cross and their typical energy separation. Analysis of the first principle calculations for both As and Se based 122 compounds indicates that this width is varying between zero (unless spin-orbit interaction is taken into account) and a number of the order of 1. Thus, the effect of the nodal lines on thermodynamical properties is comparable to that in one-band d -wave superconductors such as cuprates and therefore should be easily detectable.

Let us now gradually turn on the k_z dispersion. Nothing changes for $k_z = \pi/2c$, that is, there are four equidis-

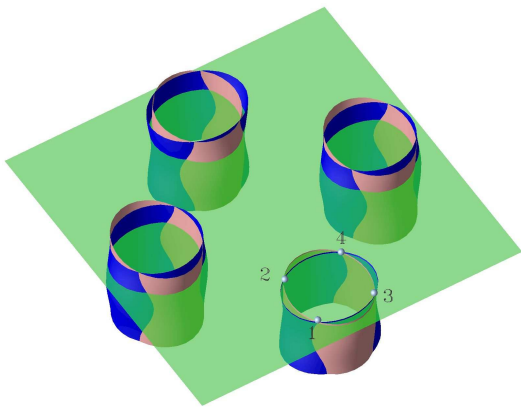


FIG. 3. Same as Fig. 2, but assuming a moderated k_z dispersion. The plane at $k_z = \pi/2c$ is shown, and one of the Fermi surfaces is clipped above this plane to show how the nodal points move away from their high symmetry positions.

tant nodes in this plane, which we can label as 1, 2, 3 and 4. As we move towards $k_z = 0$, nodes 1 and 2 get closer to each other, and so do nodes 3 and 4. As we move towards $k_z = \pi/c$, the other pairs get closer, nodes 1 and 4, and nodes 2 and 3. Thus, instead of four vertical node lines we get four wiggly lines, otherwise similar in properties to the pure 2D case in Fig. 3. Averaged over all k_z , they still have the fourfold symmetry and the observable properties should be very similar to the 2D case. A notable exception is ARPES. That technique should detect gap nodes along the (0,1) and (1,0) direction when probing $k_z = \pi/2c$, which should gradually shift away from these directions when the probed momentum is different.

This is actually the case in density functional calculations for the stoichiometric compounds in the reported crystal structure; the intersection lines of the two FSs folded on top of each other never close, and a d -wave superconductivity in this system must retain all four vertical node lines. Suppose however that these calculations underestimate the k_z dispersion (this is somewhat unlikely, as band structure calculations tend to produce too diffuse orbitals and too much hopping, but let us assume for the sake of generality that this is possible). In that case, at some finite value of \tilde{k}_z such that $0 < \tilde{k}_z < \pi/2c$ nodes 1 and 2 will merge and annihilate, and so will nodes 3 and 4, while at $k_z = \pi - \tilde{k}_z$ the other two pairs will annihilate. As a result, we will have a *horizontal* wiggly node line, the less wiggly the stronger is the 3D dispersion (Fig. 4). Importantly, a full node line remains present in any band structure, whatever assumption one makes about the 3D dispersion and ellipticity. *Thus, the fact that fully developed node lines are inconsistent with numerous reported experiments excludes a d -wave pairing as a viable possibility.*

An interesting alternative presents itself if we look closely at the calculated ab-initio Fermi surfaces of KFe_2Se_2 . One feature that distinguishes them from those in As-based materials is a very small ellipticity

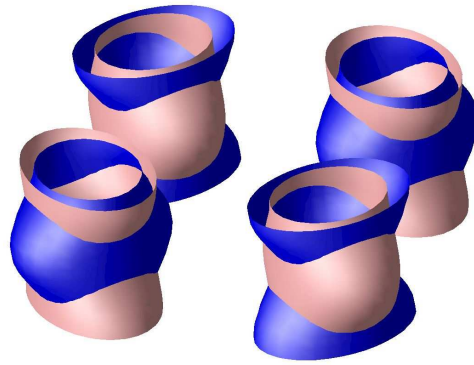


FIG. 4. Same as Fig. 3, but assuming a *very strong* k_z dispersion.

and, compared to the As-based 122 family, very little k_z dispersion¹⁸. Looking at the constant- k_z cuts (Fig. 5) of the Fermi surface, we observe that we are in a regime where the separation of the two FSs is comparable with, or smaller than the hybridization. In this case, a reasonable approximation would be to neglect both ellipticity and k_z -dispersion, and analyze the possible superconducting symmetry in this model. First of all in this approximation the resulting FSs are two concentric cylinders that touch at $k_z = 0$ but are split otherwise. The wave functions on these cylinders are, respectively, the odd and the even combinations of the original and the downfolded bands.

Thus, if the pairing interaction in the unfolded BZ exists only in the interband (interpocket) channel, as is implicitly or explicitly assumed in most current theories, it becomes identically zero after downfolding and hybridization. In fact, in this limit, when hybridization is strong everywhere in the BZ, the spin susceptibility and the pairing interaction must be computed from scratch using the 2-Fe unit cell (and the folded BZ).

Importantly, one can easily imagine an interaction that would lead to a *nodeless* state in such a system. Indeed, if the interaction is stronger between the bonding and antibonding band, than between different points in the same band, the resulting interaction will again be a sign-changing s -wave, with all inner barrels having one sign of the order parameter, and the other the opposite sign (A very similar state was unsuccessfully proposed for bilayer cuprates 15 years ago¹⁹).

Naively, one may think that one can construct a d -wave state where the signs of the order parameter will be swapped as one goes around from one M point in the BZ to another. Yet this is not allowed by symmetry, for $(2\pi/a, 0, \pi/c)$ and $(0, 2\pi/b, \pi/c)$ (2 Fe/cell notations) are reciprocal lattice vectors, so translating by any of these vectors must retain both the amplitude and the phase of the superconducting order parameter. Incidentally, this symmetry requirement is not always appreciated, and there have been “ d -wave” suggestions (*e.g.*,

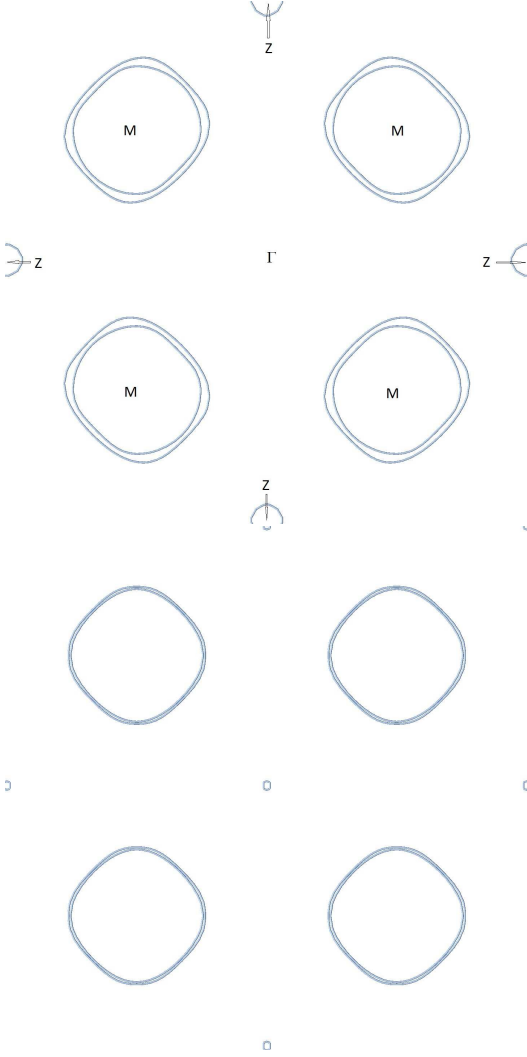


FIG. 5. Cuts of the Fermi surfaces calculated for $K_{0.8}Fe_2Se_2$ using LAPW band structure, and the experimental lattice parameter and atomic positions. Upper panel: $k_z = 0$. Lower panel: $k_z = \pi/2c$ (half way between Γ and Z).

Ref.¹⁰) that violate it.

Let us now discuss possible magnetic interactions in this system. Both from the Fermiology point of view and from experiment¹³ it is clear that familiar spin fluctuations with the wave vector $(\pi/a, \pi/b, q_z)$ are absent in this system. As discussed above, model calculations based on an unfolded band structure are much less well justified than in the old pnictides, at least if one believes the band structure calculations. In principle, one can controllably calculate the spin response using the full density functional theory²⁰, however, there are no codes widely available that are implementing such capability.

On the other hand, one can gain some insight regarding the DFT spin response at $q = 0$, in particular, on the relative strength of the fluctuations in the FM and in the AFM (checkerboard) channels, in a different way. To this

TABLE I. Calculated energies (the nonmagnetic state is taken as zero) for various stable and metastable magnetic states of KFe_2Se_2 .

	M_{Fe}, μ_B	$\Delta E, \text{meV/Fe}$
FM (LDA)	2.8	+13
FM (GGA)	2.9	-140
AFM-cb (LDA)	1.8	-111
AFM-cb (GGA)	2.1	-192
stripe (LDA)	2.2	-169
stripe (GGA)	2.4	-290

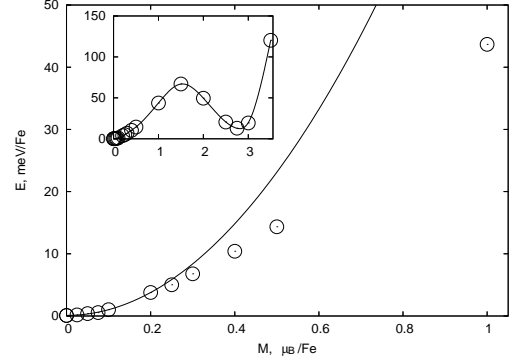


FIG. 6. Fixed spin moment calculations for the uniform (ferromagnetic) susceptibility in KFe_2Se_2 .

end, let us write the full spin susceptibility in the the local density functional theory²¹:

$$\chi^{FM} = \frac{\chi_0^{FM}}{1 - I\chi_0^{FM}}, \quad \chi^{AFM} = \frac{\chi_0^{AFM}}{1 - I\chi_0^{AFM}}, \quad (1)$$

where $I = 2\delta^2 E_{xc}/\delta M_{Fe}^2$ is the iron Stoner factor, which we, as the first approximation, will consider independent of the magnetic pattern. Note that spin-unrestricted calculations for all magnetic patterns, ferromagnetic, checkerboard, or the stripe phase similar to ferropnictides converge to large magnetic moment solutions not helpful in analyzing the linear response of the nonmagnetic phase (Table 1).

To circumvent this problem, we will use a modification of the standard LAPW package "WIEN2k", which allows for a phenomenological account of itinerant spin fluctuations by tuning the Hund's rule coupling²³. It appears that the unaltered LDA (and even GGA) functional solution in the nonmagnetic phase is stable against weak FM perturbations (Fig. 6), even though it is unstable against formation of a large magnetic moment²². It requires scaling I up by 40% to make it unstable, thus $\chi_0^{FM} \approx 1/(1.4I) = 0.7I$. at the same time, scaling I down by $\alpha \approx 0.7$, we make the checkerboard pattern also marginally stable, thus $\chi_0^{AFM} \approx 1/(0.7I) \approx 2\chi_0^{FM}$. Thus, the Fermiology favors the checkerboard antiferromagnetic fluctuations about twice more than the ferromagnetic ones.

This is in some sense encouraging. If both FM and AFM fluctuations are present, they can actually provide coupling between the bonding and antibonding sheets of the folded Fermi surface, even if the hybridization is very strong (if only AFM fluctuations are present, this coupling vanishes in the limit of strong hybridization). It may or may not be stronger than the intraband coupling. Only full calculations of susceptibility in the two Fe unit cell will give us the answer. Yet, we can firmly conclude that the only state compatible with two experimental observations, (1) that the superconducting gap does not have nodes and (2) that superconductivity emerges in immediate proximity of an ordered magnetic phase, is again an s_{\pm} state, but this time with the order parameter changing sign between the bonding and antibonding state. It is also worth noting that if a 3D electron pocket is present at Γ , as calculations and several ARPES experiments suggest, in the proposed d -wave symmetry^{8–10} it would be cut by four nodal lines which would also have been seen in the experiment. The concentric s_{\pm} state discussed above does not require any nodes on this pocket.

Finally, a word of caution is in place. While it is useful, and, arguably, imperative, at this point of time, to establish the symmetry restrictions on possible order pa-

rameter in AFe_2Se_2 compounds, the experimental situation is by far not clear. The compositions reported range from ~ 0.8 hole/Fe doped ($\text{K}_{0.65}\text{Fe}_{1.41}\text{Se}_2$, Ref.²⁴), compared to the stoichiometric AFe_2Se_2 , to ~ 0.9 electron/Fe ($\text{Tl}_{0.63}\text{K}_{0.37}\text{Fe}_{1.78}\text{Se}_2$, Ref.⁷). Se-deficient samples have also been reported²⁵. There have been credible reports about particular ordering of vacancies²⁶. Yet, the superconducting properties seem to be remarkably similar. Is it fortuitous that ARPES finds electronic structures remarkably similar to those computed for stoichiometric compounds, despite large deviations from stoichiometry? More experiments will be needed before we can gain quantitative understanding. Yet the statements based solely on crystallographic symmetry, and most of the conclusions of this paper belong to this class, should hold, and have to be kept in mind.

ACKNOWLEDGMENTS

I acknowledge discussions with Andrey Chubukov, Sigfried Graser, Peter Hirschfeld, and Douglas Scalapino. I am particularly thankful to Ole Andersen and Lilia Boeri for helping me figure out the factors that control the ellipticity and the k_z -dispersion in the 122 structure.

-
- ¹ Jiangang Guo, Shifeng Jin, Gang Wang, Shunchong Wang, Kaixing Zhu, Tingting Zhou, Meng He, and Xiaolong Chen, Superconductivity in the iron selenide $\text{K}_x\text{Fe}_2\text{Se}_2$ ($0 \leq x \leq 1.0$), *Phys. Rev. B* **82**, 180520 (2010)
 - ² Lei Fang, Huiqian Luo, Peng Cheng, Zhaosheng Wang, Ying Jia, Gang Mu, Bing Shen, I. I. Mazin, Lei Shan, Cong Ren, and Hai-Hu Wen, Roles of multiband effects and electron-hole asymmetry in the superconductivity and normal-state properties of $\text{Ba}(\text{Fe}_{1-x}\text{Co}_x)_2\text{As}_2$, *Phys. Rev. B* **80**, 140508 (2009).
 - ³ V. Brouet, M. Marsi, B. Mansart, A. Nicolaou, A. Taleb-Ibrahimi, P. Le Fèvre, F. Bertran, F. Rullier-Albenque, A. Forget, and D. Colson, Nesting between hole and electron pockets in $\text{Ba}(\text{Fe}_{1-x}\text{Co}_x)_2\text{As}_2$ ($x=0-0.3$) observed with angle-resolved photoemission, *Phys. Rev. B* **80**, 165115 (2009).
 - ⁴ I.R. Shein, A.L. Ivanovskii, Electronic structure and Fermi surface of new K intercalated iron selenide superconductor $\text{K}_x\text{Fe}_2\text{Se}_2$, arXiv:1012.5164; Chao Cao and Jianhui Dai, Electronic Structure of KFe_2Se_2 from First-Principles Calculations, arXiv:1012.5621; I.A. Nekrasov, M.V. Sadovskii, Electronic Structure, Topological Phase Transitions and Superconductivity in $(\text{K,Cs})_x\text{Fe}_2\text{Se}_2$, *Pisma ZhETF* **93**, 182 (2011).
 - ⁵ T. Qian, X.-P. Wang, W.-C. Jin, P. Zhang, P. Richard, G. Xu, X. Dai, Z. Fang, J.-G. Guo, X.-L. Chen, H. Ding, Absence of holelike Fermi surface in superconducting $\text{K}_{0.8}\text{Fe}_{1.7}\text{Se}_2$ revealed by ARPES, arXiv:1012.6017
 - ⁶ Y. Zhang, L. X. Yang, M. Xu, Z. R. Ye, F. Chen, C. He, J. Jiang, B.P. Xie, J. J. Ying, X. F. Wang, X. H. Chen, J. P. Hu, and D. L. Feng, Heavily electron-doped electronic structure and isotropic superconducting gap in $\text{A}_x\text{Fe}_2\text{Se}_2$ ($\text{A}=\text{K,Cs}$), arXiv:1012.6017.
 - ⁷ X.-P. Wang, T. Qian, P. Richard, P. Zhang, J. Dong, H.-D. Wang, C.-H. Dong, M.-H. Fang, H. Ding, Strong nodeless pairing on separate electron Fermi surface sheets in $(\text{Tl, K})\text{Fe}_{1.78}\text{Se}_2$ probed by ARPES, arXiv:1101.4923
 - ⁸ T.A. Maier, S. Graser, P.J. Hirschfeld, D.J. Scalapino, d-wave pairing from spin fluctuations in the $\text{K}_x\text{Fe}_{2-y}\text{Se}_2$ superconductors, arXiv:1101.4988
 - ⁹ Fa Wang, Fan Yang, Miao Gao, Zhong-Yi Lu, Tao Xiang, Dung-Hai Lee, The Electron Pairing of $\text{K}_x\text{Fe}_{2-y}\text{Se}_2$, arXiv:1101.4390.
 - ¹⁰ Tanmoy Das, A. V. Balatsky. Stripes, spin resonance and $d_{x^2-y^2}$ -pairing symmetry in FeSe-based layered superconductors, arXiv:1101.6056
 - ¹¹ K. Kuroki, S. Onari, R. Arita, H. Usui, Y. Tanaka, H. Kontani, and H. Aoki, *Phys. Rev. Lett.* **101**, 087004 (2008)
 - ¹² Bin Zeng, Bing Shen, Genfu Chen, Jianbao He, Duming Wang, Chunhong Li, Hai-Hu Wen, Nodeless superconductivity in $\text{K}_x\text{Fe}_{2-y}\text{Se}_2$ single crystals revealed by low temperature specific heat, arXiv:1101.5117.
 - ¹³ L. Ma, J.B. He, D.M. Wang, G.F. Chen, and W. Yu, ⁷⁷Se NMR Evidence of Strongly Coupled Superconductivity in $\text{K}_{0.8}\text{Fe}_{2-x}\text{Se}_2$, arXiv:11101.3687
 - ¹⁴ R. H. Yuan, T. Dong, G. F. Chen, J. B. He, D. M. Wang, N. L. Wang, Observation of a small superconducting energy gap in $\text{K}_{0.7}\text{Fe}_{1.8}\text{Se}_2$ by optical spectroscopy, arXiv:1102.1381.
 - ¹⁵ P.A. Lee and X.-G. Wen, *Phys. Rev. B* **78**, 144517 (2008).
 - ¹⁶ O.K. Andersen and L. Boeri, On the multi-orbital band structure and itinerant magnetism of iron-based superconductors. *Ann. der Phys.* **523**, 8 (2011).

- ¹⁷ Doubling of a unit cell and corresponding downfolding of the BZ does not necessarily lead to formation of nodes. However, it was shown by D. Parker, M. G. Vavilov, A. V. Chubukov, and I. I. Mazin (Coexistence of superconductivity and a spin-density wave in pnictide superconductors: Gap symmetry and nodal lines, Phys. Rev. **B80**, 100508, 2009), that if the symmetry lowering occurs in the charge channel (charge density wave), hybridization of bands with the opposite signs of the order parameter leads to gap nodes, while if it occurs in the spin channel the nodes are avoided. Symmetry lowering due to the Se ions occurs in the charge channel and thus nodal lines are necessarily formed.
- ¹⁸ This is true for my own calculations, which were performed in the experimental crystal structure using the standard WIEN2k band structure package, as well as for other reported calculations⁴, although pseudopotential calculations reported in Ref.⁸ have a somewhat stronger k_z dispersion.
- ¹⁹ I.I. Mazin, and O.K. Andersen, s -wave superconductivity from antiferromagnetic spin fluctuation model for $\text{YBa}_2\text{Cu}_3\text{O}_7$, A.I.Liechtenstein, I.I. Mazin, and O.K. Andersen, Phys. Rev. Lett. **74**, 2303 (1995).
- ²⁰ S.Y. Savrasov, Linear Response Calculations of Spin Fluctuations, Phys. Rev. Lett. **81**, 2570 (1998).
- ²¹ There are a number of simplifications in this expression, for instance, we have neglected the so-called local field effects and possible \mathbf{q} -dependence of the Stoner factor J , but these simplifications are not principal for our qualitative estimate.
- ²² Incidentally, the same is true for the “stripe” phase, the pattern that is the ground state in our calculations and is observed experimentally in pnictides. While the large-moment solution is very stable, the nonmagnetic state is stable against small perturbations of this symmetry, not only is LDA but also in GGA.
- ²³ This is implemented by the following recipe: first, at each iteration, the standard LDA or GGA potential for the spin-up and spin-down channel is calculated; then, it is rescaled according to formula $v_\uparrow(\mathbf{r}) = [v_\uparrow(\mathbf{r}) + v_\downarrow(\mathbf{r})]/2 + \alpha[v_\uparrow(\mathbf{r}) - v_\downarrow(\mathbf{r})]/2 = v_\uparrow(\mathbf{r})(1 + \alpha)/2 + v_\downarrow(\mathbf{r})(1 - \alpha)/2$, $v_\downarrow(\mathbf{r}) = v_\uparrow(\mathbf{r})(1 - \alpha)/2 + v_\downarrow(\mathbf{r})(1 + \alpha)/2$, where $0 \leq \alpha \leq 1$.
- ²⁴ D. A. Torchetti, M. Fu, D. C. Christensen, K. J. Nelson, T. Imai, H. C. Lei, C. Petrovic, ⁷⁷Se NMR Investigation of the $\text{K}_x\text{Fe}_{2-y}\text{Se}_2$ High T_c Superconductor ($T_c=33$ K), arXiv:1101.4967.
- ²⁵ J. J. Ying, X. F. Wang, X. G. Luo, A. F. Wang, M. Zhang, Y. J. Yan, Z. J. Xiang, R. H. Liu, P. Cheng, G. J. Ye and X. H. Chen, Superconductivity and Magnetic Properties of high-quality single crystals of $\text{A}_x\text{Fe}_2\text{Se}_2$ ($\text{A} = \text{K}$ and Cs), arXiv:1012.5552
- ²⁶ P. Zavalij, W. Bao, X. F. Wang, J. J. Ying, X. H. Chen, D. M. Wang, J. B. He, X. Q. Wang, G.F. Chen, P-Y Hsieh, Q. Huang, M. A. Green, On the Structure of Vacancy Ordered Superconducting Potassium Iron Selenide, arXiv:1101.4882; J. Bacsá, A.Y. Ganin, Y. Takabayashi, K.E. Christensen, K. Prassides, M.J. Rosseinsky, J.B. Claridge, Cation vacancy order in the $\text{K}_{0.8+x}\text{Fe}_{1.6-y}\text{Se}_2$ system: five-fold cell expansion accommodates 20% tetrahedral vacancies, arXiv:1102.0488.